

Nectarine Coated with Biopolymeric Nanocapsules Containing Eugenol to Control Brown Rot

Joslaine Jacumazo,^{a,b} Gabriela P. Parchen,^a Meira J. B. Garcia,^{b,c} Nayana C. S. Santos,^b
Louise L. M. De Mio,^c Francisco A. Marques^{ib} and Rilton A. de Freitas^{ib}*,^a

^aLaboratório de BioPolímeros (BIOPOL), Departamento de Química, Universidade Federal do Paraná (UFPR),
R. Coronel F. H. dos Santos, 210, 81531-980 Curitiba-PR, Brazil

^bLaboratório de Ecologia Química e Síntese de Produtos Naturais (LECOSIN), Departamento de Química,
Universidade Federal do Paraná (UFPR), R. Coronel F. H. dos Santos, 210, 81531-980 Curitiba-PR, Brazil

^cLaboratório de Epidemiologia para Manejo Integrado de Doenças de Plantas (LEMID),
Departamento de Agronomia, Universidade Federal do Paraná (UFPR),
R. dos Funcionários, 1540, 80035-050 Curitiba-PR, Brazil

Infections in fruits caused by fungi reduce the quantity and quality of food for human consumption, in addition to causing economic losses. In this sense, this study aimed to address the effects of eugenol nanocapsules (NCs) based on chitosan and carboxymethylcellulose in protecting nectarines against *Monilinia fructicola*, a brown rot agent, a worldwide important disease. NCs were prepared by layer-by-layer (LbL) self-assembly starting from an anionic template and deposition with up to two polymeric layers. The hydrodynamic diameters ranged from 158 nm (nanoemulsion), 360 nm (one polymeric layer) to 398 nm (two polymeric layers). NCs presented, during the *in vitro* release, the release of eugenol following a first order process. In addition to being in the region of stability (zeta potential ca. 130 mV), the capsules showed good adhesion to the nectarine surface. In relation to brown rot, the eugenol NCs with chitosan proved to be the best formulation compared to nanoemulsion and NCs with two polymeric layers for its control, increasing the probability that the fruits remain without symptoms, even after 7 days. Therefore, this study demonstrated that chitosan NCs containing eugenol could be an alternative to preserve fruit for longer periods in post-harvest.

Keywords: biopolymers, layer-by-layer, adhesion, eugenol, *Monilinia fructicola*, disease control

Introduction

Fruits are an essential part of a healthy diet for humans due to their composition based on minor components such as vitamins, minerals, and fibers.¹ Nectarine (*Prunus persica* var. *nucipersica*) is a popular fruit and highly nutrient, belonging to the Rosaceae family. The worldwide nectarine and peach production in 2019 reached 22.3 million tons. However, due to its typical climacteric properties, the fruit ripens quickly under environmental conditions, and after harvesting there is an increase in the production of plant hormone ethylene, which is responsible for its ripening and, therefore, limiting the storage time in the post-harvest. This condition affects the fruit characteristics such as the

decrease in firmness, in addition to the loss of color and flavor.^{2,3} Furthermore, under these circumstances, infection by microorganisms such as fungi may occur.

Brown rot is one of the main diseases that affect nectarine.⁴ This disease is caused by the fungi *Monilinia fructicola* (Wint) Honey. This pathogen is responsible for infecting the plant during the blossom time and during the fruit grown stage.⁴⁻⁶ It can remain in the fruit latently, showing symptoms only when the environment becomes favorable, for example, in the post-harvest. Chemical control methods are still predominantly using fungicides, reducing the loss to 5-10% in the post-harvest. However, this microorganism has been associated to resistance to fungicides.^{4,6-9}

Clove essential oils, composed mainly of eugenol (45-90%), are highlighted as promisor green preservative for foods.^{10,11} Eugenol can control plant pathogens, presenting a fungitoxic mode of action.¹²

*e-mail: rilton@ufpr.br

Editor handled this article: Paulo Cezar Vieira

The biggest limitation associated with the application of eugenol as a green preservative is the volatility, low solubility in water and degradation by light and oxygen.^{13,14} To overcome these difficulties, nanoencapsulation has become an interesting and promising alternative.¹⁵ Nanoencapsulation can be obtained by various methods, including nanoprecipitation, emulsion-diffusion, coacervation, and layer-by-layer (LbL).¹⁶

Chitosan, as an example of biopolymer for LbL, presents excellent biocompatibility and biodegradability, making it an ideal alternative for interaction with other polymers and to develop nanocapsules (NCs).^{17,18} Carboxymethylcellulose is a negative charged polymer, biodegradable and non-toxic that can interact ionically with chitosan, by a LbL process.¹⁹

As presented, encapsulation could be a good strategy to increase the shelf-life of products, and in this work, the LbL technique was used to prepare NCs containing eugenol, as a green preservative. Two edible polysaccharides, chitosan and carboxymethylcellulose, were used to develop a modified release fruit coating system to control the pathogenic fungi. Our hypothesis is that by coating nectarine with eugenol nanocapsules the incidence of brown rot caused by *Monilinia fructicola* could be reduced. In this article, nectarine surfaces were exposed to a challenge test: contamination using *Monilinia fructicola*. This strategy offers new perspectives to increase fruit quality and to reduce post-harvest losses.

Experimental

Chemicals

Chitosan ($C_6H_{11}NO_4$)_n was purchased from Shangyu Biotech Co, Ltda (Shangyu, China) and submitted to a purification procedure before use, as described in previous work.²⁰ The chitosan average molar mass (M_w) was 1.9×10^5 g mol⁻¹ with deacetylation degree (DD) of 76%. Sodium dodecyl sulphate (99.0 wt.% purity), eugenol (99.0% v v⁻¹ purity), formamide (99.5% v v⁻¹ purity) and 2,2-diphenyl-1-picryl-hydrazil (DPPH) were purchased from Sigma-Aldrich (St. Louis, USA). Diiodomethane (99.0% v v⁻¹ purity) was purchased from Neon (Suzano, Brazil). Carboxymethylcellulose with M_w of 6.7×10^5 g mol⁻¹ and carboxymethyl degree of substitution (DS) of 0.84 was purchased from Acros Organics (Geel, Belgium). All solutions were prepared with purified water obtained by a reverse osmosis system.

The nectarines (*Prunus persica* var. nucipersica), Sungold variety, were obtained at Paraná Supply Center in Curitiba (CEASA) from Santa Catarina, Brazil.

Nanoemulsion of eugenol

Nanoemulsions of eugenol (Ne) were obtained from the addition of eugenol in a sodium dodecyl sulfate solution (5.0 mmol L⁻¹), the eugenol:sodium dodecyl sulfate ratio was 0.78:1 m v⁻¹. This mixture was sonicated (Ultrasonics Sonicator, Virginia, USA) at 30% amplitude, 750 W and 20 kHz. The time of sonication varied from 30, 120, 240, 360, 480 to 600 s at 0 °C. At the end of the sonication process, Ne was left under magnetic stirring at 900 rpm (Magnetic Agitator MAG15, Marte Scientific, São Paulo, Brazil) for 15 min.

Layer-by-layer of eugenol-loaded nanocapsules

LbL technique was used for the self-assembly of polymer layers.²⁰ Polymeric dispersions of chitosan (2 mg mL⁻¹), carboxymethylcellulose (2 mg mL⁻¹), and Ne were performed in sodium acetate buffer (0.01 mol L⁻¹, pH 4.6). Self-assembly step was performed in two different situations: in condition 1 (C1), the polymer dispersion was added into the Ne; and condition 2 (C2), the Ne was added into the polymer dispersion. From the Ne, the NCs were formed by alternating deposition of the polymer: cationic (Ne-LbL₁ NCs) and anionic (Ne-LbL₂ NCs), using direct mixture of equal volumes of each dispersion at 25 °C and stirring at 900 rpm during 1 h. After each polymer deposition, the nanocapsules were centrifuged (5×10^4 g, 30 min) at 25 °C, washed with water, and kept under continuous magnetic stirring at 900 rpm, 25 °C for 1 h after resuspension.

Using the same protocol, eugenol free particles were produced as controls for antimicrobial assays and named LbL₁ NCs and LbL₂ NCs.

Eugenol-loaded nanocapsules characterization

Average apparent hydrodynamic diameter (D_{app}) was determined using a dynamic light scattering (DLS) on a NANO DLS Particle Size Analyzer apparatus of Brookhaven Instruments (Holtsville, New York, USA) in water at 20 °C. All experiments were conducted using a 15 mW solid-state He-Ne laser, operating at 90° and 632.8 nm. Samples containing the NCs were diluted in purified water 1:50 (v v⁻¹).

Zeta potential (ζ -potential) analyses were carried out in a Particle Charge Mapping Stabino apparatus (Meerbusch, Germany). Samples were diluted in water 1:50 (v v⁻¹) and analyzed for 100 s at 20 °C.

Thermogravimetric (TG) analysis intending to confirm the release of eugenol from the NCs was performed with of eugenol (6.1 mg), chitosan and carboxymethylcellulose

mixture (5.2 mg), Ne-LbL₁ NCs (4.9 mg), Ne-LbL₂ NCs (4.6 mg) were performed using 0.065 mL alumina crucibles with a Netzsch analyzer (STA 449 F3 series EP), following a heating rate at 10 °C min⁻¹ from 25 to 600 °C under nitrogen atmosphere of 50 mL min⁻¹. The NCs with eugenol were previously lyophilized at -50 °C (MicroModulyo, Thermo Electron Corporation, USA) prior to the TG analysis.

Encapsulation efficiency and *in vitro* release

Encapsulation efficiency (EE%) of eugenol was determined according to the method described by Jacumazo *et al.*²⁰ Solubility of eugenol in water and chloroform was determined using spectroscopy in the UV-Vis region (281 nm) and the values were 2.41 and 8.18 g L⁻¹, respectively. Samples (2 mL) were centrifuged (4.000 g, 15 min) at 5 °C. Supernatant was removed, and chloroform (2 mL) was added to the sedimented material, mixed, and centrifuged (4.000 g, 20 min) at 25 °C. Supernatant was collected, and absorbance was measured at 281 nm using UV-Vis spectrophotometry. Experiments were run in triplicate.

Eugenol release experiments were measured using a dialyze procedure. Samples were added to a cellulose dialysis bag (cut-off of 12 kg mol⁻¹, D0530-100FT, Sigma-Aldrich, Germany, USA) and then placed in the receptor system containing water. Saturation concentration of eugenol in water was 69.8 mg L⁻¹, and all the experiments were maintained under sink conditions. Experiment was performed at pH 6.8, 25 °C, and continuous magnetic stirring (900 rpm) for 96 h. At defined time intervals (0, 0.25, 0.5, 1, 2, 3, 4, 5, 24, 48, 72, and 96 h), an aliquot of 2 mL of the receptor medium was collected and analyzed using a UV-Vis spectrophotometer in the wavelength of 281 nm. Medium receptor was immediately replenished with equal volumes of water. The experiments were run in triplicate. Eugenol quantification was estimated using an equation of the analytical curve, with R₂ (coefficient of determination) = 0.998, Eugenol / (mg L⁻¹) = $\left(\frac{\text{absorbance} - 0.011}{0.015 \text{ L mg}^{-1}} \right)$, and the limits of detection and quantification were 0.40 and 1.34 mg L⁻¹, respectively.

A first-order equation was used to adjust the release of eugenol. In equation 1, represents the fraction released at time t, is the amount of the active in the formulation, and k is the first-order constant.

$$\ln\left(\frac{m_t}{m_\infty}\right) = kt \quad (1)$$

Nectarine coating from nanocapsules

Preparation

Nectarine coating was carried out with the Ne-LbL₁ NCs and Ne-LbL₂ NCs, and nectarine without coating was used as control. The nectarines were placed in contact with the dispersions (Ne-LbL₁₋₂ NCs) or distilled water (control) for 30 s and then dried at 25 °C for 24 h. After drying, the nectarine peel was withdrawn, and the contact angle analysis was performed in duplicate with six drops *per* sample.

Characterization: contact angle, surface free energy, and adhesion work

Contact angle measurements were performed using three liquids: water, formamide, and diiodomethane, and measured at 20 °C using a DATAPHYSICS Instruments GmbH Contact Angle System OCA15+ tensiometer (Filderstadt, Germany). Contact angle at the nectarine surface was measured by the sessile drop method, and 5 µL of each liquid was dripped on the samples. The right and left side of the drop was measured to average the contact angle. Contact angles were automatically calculated by fitting the captured drop shape (software SCA20).

Calculation of the surface energy of the nectarine coating was based on the method described by Owens and Wendt²¹ (1969) and Kaelble²² (1970), using the Owens, Wendt, Rabel, and Kaelble (OWRK) method to calculate the components of the solid surface energy and performed using equation 2.

$$\frac{\gamma_L (\cos\theta_c + 1)}{2(\sqrt{\gamma_L^D})} = \sqrt{\gamma_S^P} \left(\frac{\sqrt{\gamma_L^P}}{\sqrt{\gamma_L^D}} \right) + \sqrt{\gamma_S^D} \quad (2)$$

where θ_c is the experimental contact angle, γ_L is the total liquid surface tension, γ^D is the dispersive component, γ^P is the polar component, S and L stand for solid and liquid, respectively.

Work of adhesion of LbL₁ NCs and Ne-LbL₁ NCs with the nectarine surface, as well as the LbL₂ NCs with the chitosan layer (LbL₁), was calculated using equations 3, 4 and 5.

$$W_a = W_a^P + W_a^D \quad (3)$$

$$W_a^P = 2\sqrt{\gamma_x^P \gamma_y^P} \quad (4)$$

$$W_a^D = 2\sqrt{\gamma_x^D \gamma_y^D} \quad (5)$$

where $W_{a,x,y}$ is the total work of adhesion between layers x and y, and γ_x and γ_y are the free energy of the two different interfaces.

Microbial assays for brown rot control

Fungus (isolated PpMfSP15/575) from *Monilinia fructicola*, come from the LEMID-UFPR collection. The conidial suspension was prepared to collect the spores on the surface of pre-inoculated canned peach and dispersed into a sterile tween 20 (0.5% v/v) aqueous solution.

Nectarines (*Prunus persica* var. nucipersica) of Sungold cultivar (Santa Catarina, Brazil) were used in the experiment. These fruits were previously sanitized by immersion (1 min) in ethanol/water (70% v/v), an aqueous solution of sodium hypochlorite (1% v/v), and purified water (3×), and then let dry at ambient temperature (25 °C).

Nectarine fruits were treated with sterile water (control), an aqueous solution of eugenol using dimethyl sulfoxide and Adivex® as co-solvents (formulation control), NCs without eugenol, Ne-LbL_{1,2} NCs, and a fungicide efficient to control brown rot (iprodione, 500 g L⁻¹ Basf, France) as the positive control, efficient to control brown rot. Nectarines were dripped in each treatment for 30 s and dried for 24 h. Then, each nectarine was inoculated with 40 µL of the *Monilinia fructicola* conidial suspension (10⁵ conidial mL⁻¹) in the region demarked with a pen on the fruit and the samples were placed in the humid chamber. Seven repetitions were performed for each treatment and symptoms evaluations were performed every 24 h for 7 days, and the experiments were conducted twice in a completely randomized design.

Data analysis

The statistical analysis was performed with GraphPad Prism 8 software,²³ using a one-way analysis of variance (ANOVA), followed by Tukey's Post Hoc test ($p \leq 0.05$). Survival analysis was estimated by the Kaplan-Meier method and the comparison of curves between treatments was estimated by the non-parametric log-rank test. In addition, Cox's proportional hazards model was also used for all tested samples. For all statistical inferences, $p < 0.05$ was considered a nominal significance level. The statistical software R (version 3.4.3)²⁴ was used for data analysis and graphical representation. For other figures the Microcal Origin 8.0 was used.²⁵

Results and Discussion

Layer-by-layer of eugenol-loaded nanocapsules

Ne formation is an important step to obtain nanocapsules since it was used as a template for the LbL process²⁶ and in

this work, the variation of the sonication time to obtain the Ne was evaluated. Droplet size and the polydispersity index (PDI) of the Ne as a function of sonication time are shown in Figure 1a. After 240 s of sonication, there is a decrease in the droplet size and sample dispersion ($p < 0.05$). Between 30 s (PDI = 0.494) and 600 s (PDI = 0.230), there is a considerable difference ($p < 0.05$) in the dispersion due to the greater amount of energy supplied to the system Figure 1b. PDI < 0.250 suggested a more homogeneous distribution, reducing the Ostwald ripening and contributing to stability. In this context, the best condition to form homogeneous Ne droplets was determined at 600 s of sonication.

After selecting the best condition to obtain Ne, NCs were obtained by LbL, and the order of addition of the precursors could alter some final properties of the NCs, for example, the average diameter as described by Liu *et al.*²⁷ Two different ways of adding the precursor materials were followed to identify the best protocol. In condition 1 (C1), the polymeric dispersion was added over the Ne and in condition 2 (C2), the Ne was added over the polymeric dispersion.

In C1, the dispersion of chitosan, that has a positive charge in acid medium over the Ne, made the dispersion immediately milky-like (Figure 1c, C1). For this situation, the D_{app} (Figure 1c) and the PDI were 368 ± 113 nm and 0.546, respectively. The higher PDI value indicated a non-uniform formation of NCs.

For C2, the Ne was added to chitosan dispersion, and the original light-yellow dispersion color gradually became light-milky (Figure 1c, C2). In this situation, the droplet coating with chitosan molecules occurred immediately, and the D_{app} (Figure 1c) and PDI were 360 ± 30 nm and 0.390, respectively, lower than C1 ($p < 0.05$). Size and PDI variation were monitored for the other self-assembly layers. However, no significant differences were observed in D_{app} and PDI after carboxymethylcellulose addition ($p > 0.05$), and the values obtained were D_{app} : 473 ± 164 nm and PDI: 0.440 for C1 and D_{app} : 398 ± 106 nm and PDI: 0.396 for C2.

In addition to the NCs size, stability by ζ -potential was observed after each coating, for C1 and C2. In Figure 1d, it is possible to observe the zeta potential inversion for each polymeric deposition and to infer that regardless of the order of addition of the polysaccharides, the NCs are close to the stability region (ca. |30| mV).²⁸ Considering the lower PDI, further experiments were performed using the condition C2.

Encapsulation efficiency (EE%) and *in vitro* eugenol release from nanocapsules

EE of eugenol was determined as $8.3 \pm 0.1\%$ for Ne-LbL₁ NCs and $5.1 \pm 0.3\%$ for Ne-LbL₂ NCs. EE

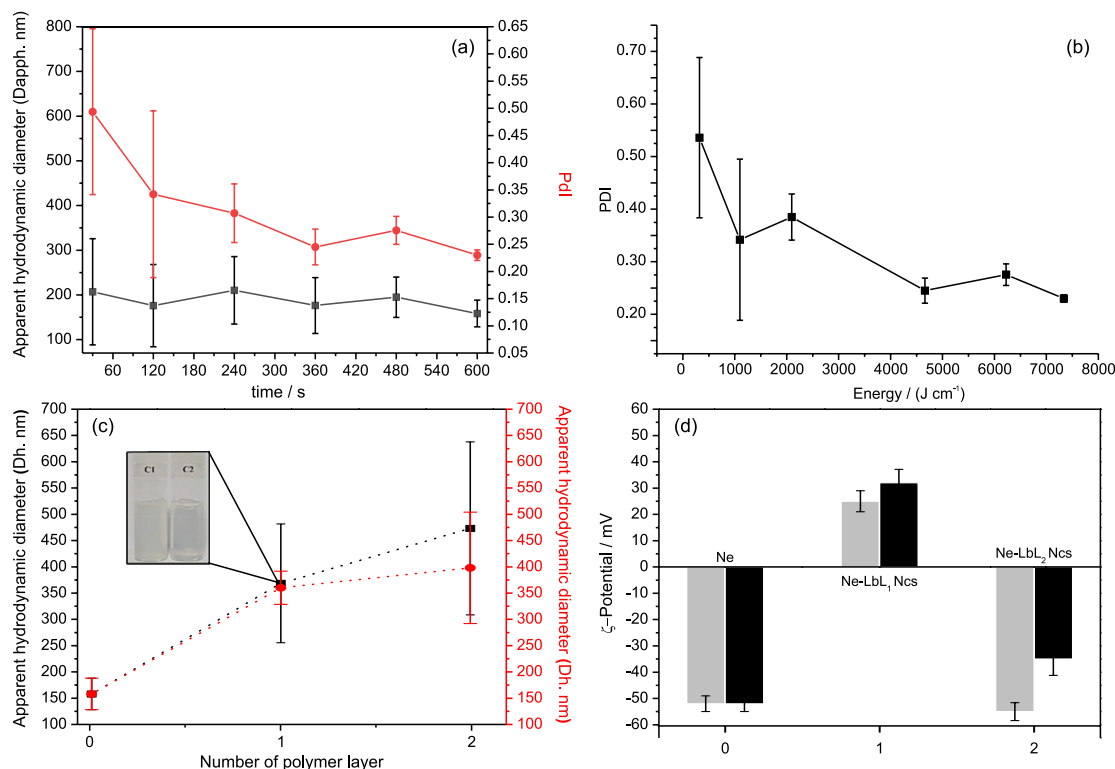


Figure 1. (a) Effect of different sonication times on the (■) D_{apph} and (●) PDI of samples at condition 1 (C1) and condition (C2); (b) changes in PDI versus energy applied (■); average D_{apph} of NCs with polymeric layer number (c) condition 1 (C1): polymer over the Ne (■) and condition 2 (C2): Ne over the polymer (●); (d) variation of the ζ -potential concerning the order of addition of precursors for condition 1 (■) and condition 2 (■). The insert in C shows the aspect on C1 and C2 condition.

apparently is dependent on the protocol used to produce the particles, depending mostly on the initial eugenol concentration. According to Jacumazo *et al.*,²⁰ similar NCs could present up to ca. 71% of eugenol, only using lower initial concentrations of eugenol. Encapsulation of eugenol was also confirmed by the thermogravimetric analysis presented in Figure S1 and by the mass losses observed in Table S1 (Supplementary Information (SI) section).

Eugenol release profile was investigated to understand the mechanism of release from NCs. Figure 2 shows for free eugenol a burst release in the first 15 min ($34 \pm 4\%$), reaching 100% ca. 4 h, in water. In contrast, for eugenol encapsulated in Ne-LbL_{1,2} the initial burst release phase is followed by a prolonged release, over an extended period of time (100 h). Release of the eugenol from Ne-LbL_{1,2} NCs was determined as a first order process, and as a concentration-dependent process.

The decrease in the release, comparing Ne-LbL₂ NCs with Ne-LbL₁ NCs, was directly related to the number of polymer layers added, as observed in previous studies.²⁰

The values of k using a first-order model for free eugenol, Ne-LbL₁ NCs and Ne-LbL₂ NCs were 0.057, 0.033, and 0.031 min⁻¹, respectively. The first-order kinetic model refers to the process where eugenol release was concentration-dependent. Also, the presence of polymeric

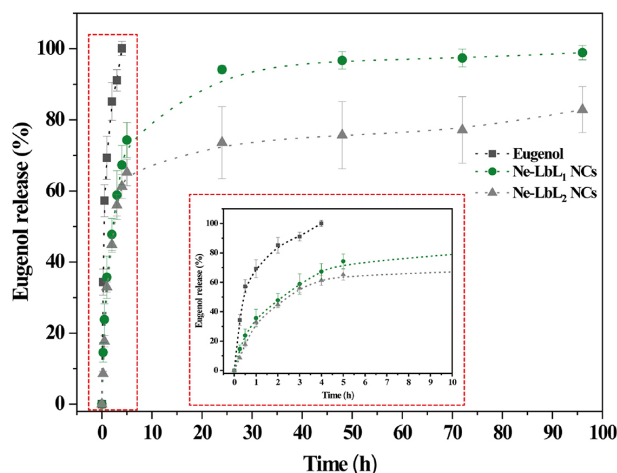


Figure 2. Release profile of (-■-) free eugenol and NCs with up to two polymeric layers (-●-) Ne-LbL₁, (-▲-) and Ne-LbL₂ NCs. The insert shows the first 5 h of experiment.

layers decreased k , due to the formation of porous layers that limit the diffusion process, but apparently is the same for one or two polymeric layers, suggesting only partial coating using carboxymethylcellulose. It can be inferred that the polymer layers reduced the eugenol diffusion and that Ne-LbL_{1,2} NCs made eugenol release slower.

Wang *et al.*²⁹ developed a self-assembled gelatin-chitosan nanocapsules as a water-soluble system for alcohol

soluble compounds, as eugenol, in which free eugenol was released fast, reaching 84% within 2 h. Similar results were observed in this article. The amount of free eugenol release was the same in our article, and for Ne-LbL_{1,2} NCs, approximately 60% of eugenol was released after 5 h, followed by a very low release stage.

NCs can be used to coat products such as fruits and vegetables by increasing their shelf life,³⁰ providing, in addition, the release of actives for protection against pathogens. In this sense, nectarine coatings were made with NCs containing eugenol. Macroscopic aspects of the coatings can be seen in Figure S2 (SI section). It is notable that after 24 h the coatings are homogeneous and transparent, and it is not possible to observe macroscopic differences concerning the control sample.

To obtain more information about these coatings, contact angle measurements of untreated nectarines (control), treated with NCs in the presence of eugenol (Ne-LbL_{1,2} NCs) and NCs in the absence of eugenol (LbL_{1,2} NCs), were performed. Contact angles were obtained using three liquids of different polarities (water, formamide, and diiodomethane) as shown in Figure 3a. Both NCs presented a comparable work of adhesion on the surface of nectarines, indicating their good wettability (Figure 3).

When the liquid drop encounters the nectarine surface, intermolecular interactions are established between the epicarp surface or film surface and the specific liquid drop, which can be attractive or repulsive forces.³¹ Thus, considering a polar liquid, the greater the contact angle, the lower the affinity of the surface in question to the liquid, that is, the more hydrophobic this surface is and the less wettable. This could be observed for the control sample when in contact with water and formamide liquids ($p < 0.05$).

On the other hand, the contact angles of the samples treated with the NCs decreased, compared to the control, increasing the wettability ($p < 0.05$). In samples with the chitosan layer, there was a greater increase in wettability compared to the other samples, possibly a better nectarine coating. This may be related to the better interaction of the chitosan acetyl groups with the nectarine, thus making the hydrophilic groups of chitosan more exposed. In the case of coating with the second layer of polymer (carboxymethylcellulose), this decrease is not so marked, this may be related to an incomplete coating as seen in Figure 3.

With the obtained contact angle values for all liquids, it was possible to calculate the values of total surface-free energy (γ^{total}), dispersive and polar components using the OWRK model. The total surface tension (γ^{total}), dispersive (γ^{D}), and polar (γ^{P}) components values for the

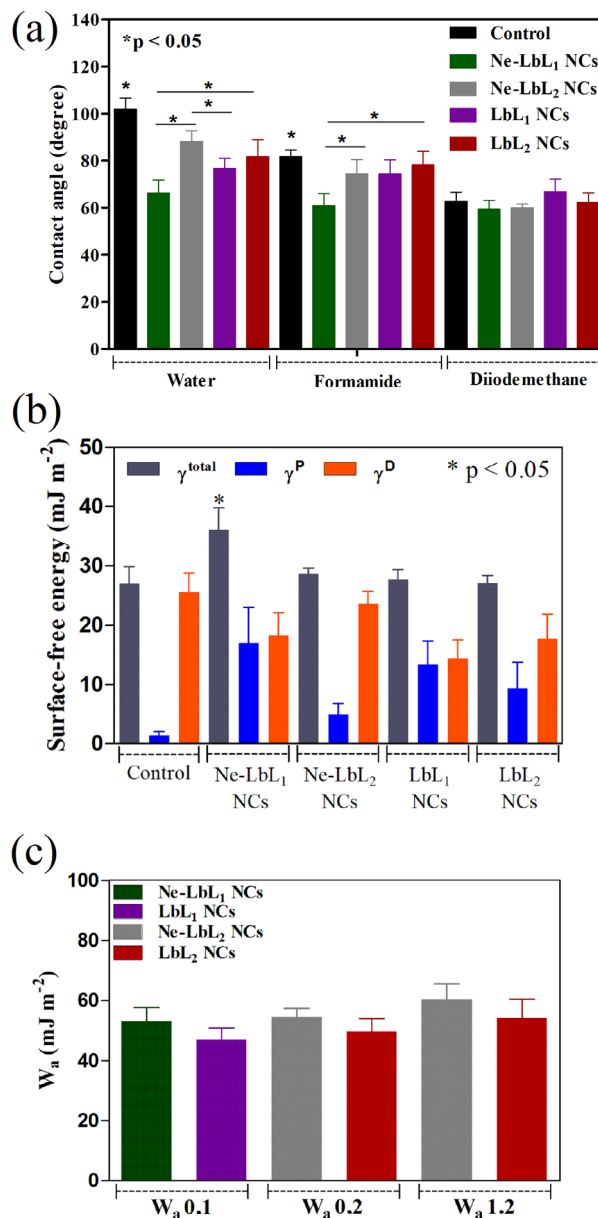


Figure 3. (a) Average values and standard deviation ($n = 6$) of contact angle of water, formamide and diiodomethane for nectarines not treated (control) and treated with Ne-LbL_{1,2} and absence of eugenol (LbL_{1,2}); (b) surface-free energy (γ^{total}), dispersive (γ^{D}) and polar (γ^{P}) components calculate by the OWRK model; (c) work of adhesion (W_a) of NCs in the absence and presence of eugenol over nectarines were 0 means the nectarine surface, 1 the film formed with particles LbL₁ and 2 LbL₂ the film formed with particles LbL₂.

three liquids used can be seen in Table S2 in the SI section. The control sample, nectarine peel treated with water, had a lower surface free energy value ($26.9 \pm 2.9 \text{ mJ m}^{-2}$) (Figure 3b), on the other hand, nectarines with Ne-LbL₁ NCs coating showed a higher total surface-free energy value ($36.1 \pm 3.7 \text{ mJ m}^{-2}$). Comparatively, the control sample has a less polar surface than LbL₁ and LbL₂ and the values of total surface-free energy were different for the untreated and treated samples with Ne-LbL₁ NCs ($p < 0.05$).

In the nectarines coated with chitosan with Ne-LbL₁NCs and LbL₁ NCs, values of 18.2 ± 3.9 and 14.3 ± 3.1 mJ m⁻² were observed respectively for the dispersive components and 17.0 ± 6 and 13.3 ± 4.1 mJ m⁻² for the polar components, where the dispersive and polar components do not differ ($p > 0.05$). After coating with LbL₁, the surface polarity increased, however, maintaining equivalent dispersive composition.

Nectarines coated with the anionic polymer, Ne-LbL₂ NCs, and LbL₂ NCs, the values of 23.6 ± 1.9 and 17.7 ± 4.1 mJ m⁻² were observed respectively for the dispersive components and 4.9 ± 1.9 and 9.3 ± 4.4 mJ m⁻² for the polar components, and the dispersive and polar components do not differ ($p > 0.05$). Ne-LbL₂ NCs have a larger dispersive component, possibly due to the strong ionic interaction between chitosan and carboxymethylcellulose and exposing less polar sites of cellulose.

With the calculated data of total surface-free energy and dispersive and polar components, it was possible to obtain the work of adhesion (W_a) (Figure 3c). As observed, the W_a determined to LbL₁ on nectarines ($W_a 0,1$), or for LbL₂ on LbL₁ ($W_a 1,2$) was almost of the same order of magnitude. It is important to highlight that both polysaccharides could be useful to coat nectarines, with almost the same W_a ($W_a 0,1$ or $W_a 0,2$). However, the LbL₁ of chitosan turns the surface much more polar than LbL₂, and this could promote interesting biological properties.

According to Velásquez *et al.*,³² the chemical composition of the wax is a mixture of long-chain compounds, including hydrocarbons, ketones, alcohols, aldehydes, and free and esterified fatty acids, the percentage of the composition varies from fruit to fruit. Lino *et al.*³³ observed that the nectarine waxes were composed of triterpenoids, mostly ursolic acid and oleanolic acids, phytosterols, and very long aliphatic chains. The authors correlated the endocarp lignification inversely with the susceptibility to *Monilinia* infection, suggesting that the triterpenoid could play a major role to control brown root infection. Thus, the components of the nectarine epicuticular wax may be promoting intermolecular interactions with the components of the NCs, chitosan and carboxymethylcellulose, and consequently promoting a physical barrier to contamination as measured by the W_a .

Effect of nanocapsules on the brown rot

In the present study, antimicrobial activity was evaluated using NCs with up to two layers of polymers containing eugenol (Ne-LbL_{1,2} NCs), aqueous solution of eugenol, NCs in absence of eugenol (LbL₁ NCs) and aqueous solution of the commonly used fungicide iprodione for the control of brown rot.³⁴

In this sense, the estimate of the relative risk for the expression of symptoms of *Monilinia fructicola* infection was analyzed using the Cox semiparametric model (Table 1) using nectarine in the absence of treatment as a standard. It is possible to observe that the nectarines coated with the NCs in the presence of eugenol, followed by the aqueous solution of eugenol were the ones that presented the lowest relative risk, therefore, the lowest probability of the fruit becoming ill. On the other hand, fruits treated with the fungicide were more susceptible to the onset of disease symptoms. Regarding the confidence interval (CI, 95%) the NCs containing eugenol and the aqueous solution of eugenol are the samples that differ from the control sample, confirming the lower risk of contamination of the fruits.

Table 1. Estimates of relative risk for the expression of symptoms of *Monilinia fructicola* estimated by the Cox semiparametric model, followed by 95% confidence intervals for nectarine

Treatment	Incubation period / days	Relative risk	CI (95%)	
			LL	US
Control	3	–	–	–
LbL ₁ NCs	4	0.7218	0.5111	1.0194
Iprodione	2	0.9272	0.6724	1.2786
Eugenol	5	0.5651	0.3918	0.8150
Ne-LbL ₁ NCs	> 7	0.2351	0.1480	0.3736
Ne-LbL ₂ NCs	5	0.4959	0.3423	0.7184

Incubation period is the number of days between the inoculation (contact of the pathogen with the nectarine fruit) and the symptoms expression on at least 50% of the sample (inoculated fruit). CI: confidence interval (95%); LL: lower limits; US: upper limit; NCs: nanocapsules.

The survival analysis of the healthy fruits is shown in Figure 4 with a study time of 7 days. It can be observed that over time there is a decrease in the probability of the fruits remaining without symptoms of brown rot for all treatments. Untreated (control) and fungicide treated nectarines, LbL₁ NCs and aqueous solution of eugenol expressed disease symptoms more rapidly than those treated with Ne-LbL_{1,2} NCs. For the control fruits and those treated with iprodione, on the fifth day, there was less than 50% probability that the fruits remained without disease symptoms.

Furthermore, the fruits treated with iprodione were the ones that showed the most symptoms of the disease, with a probability below 20% of the fruits remaining without the disease until the end of the study (7 days). In the case of fruits treated with NCs with the outer layer of chitosan, there was a higher probability of survival compared to NCs with the outer layer of carboxymethylcellulose, which corroborates the better adherence of Ne-LbL₁ NCs to nectarines, as shown in the work of adhesion

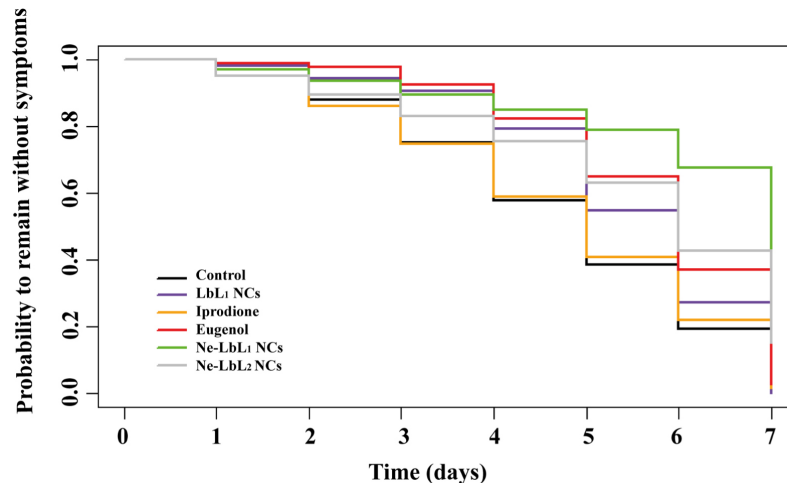


Figure 4. Estimation of Kaplan-Meier curves by survival analysis, indicating the probability over time of nectarines to remain without the occurrence of symptoms of *Monilinia fructicola* with different treatments (–) control, (–) LbL₁ NCs, (–) iprodione, (–) aqueous solution of eugenol, (–) Ne-LbL₁ and (–) Ne-LbL₂ NCs.

data. In this sense, although treatments with LbL₁ NCs, NCs with the outer layer of carboxymethylcellulose (Ne-LbL_{1,2} NCs) and aqueous solution of eugenol enable the efficient control of the pathogen *Monilinia fructicola* when compared to treatment with iprodione, only the fruits treated with NCs with the outer layer of chitosan (Ne-LbL₁ NCs) showed above 70% probability that the fruits remain in the absence of symptoms until the seventh day of the study.

Images of the experiments containing all treatments during the 7 days can be seen in Figure S3 (SI section), as some fruits showed more accentuated symptoms, they were removed from the experiment to minimize possible contamination in other fruits.

Lower brown rot control efficiency promoted by the aqueous solution of eugenol may be associated with its rapid volatilization and low stability when exposed to light, temperature, or humidity, as documented in the literature.¹³ On the other hand, its encapsulation process enabled the formation of a protective barrier to the factors mentioned above, enabling the control of the pathogen for a longer period and with a smaller amount of active, since the incorporation efficiency (IE%) of eugenol in NCs with the first polymeric coating was close at 8.3%. As a second layer of the polymer was added, there was a decrease in pathogen inhibition. This may be related to the fact that systems with lower release rates may take longer to efficiently reach the fungus, for this reason, Ne-LbL₁ NCs had the best fungicidal activity ($p < 0.05$).

In addition, the effective control of treatments containing NCs may be related to the coating that NCs promote on the surface of nectarines; this coating provides a barrier against external elements, in addition to protecting against moisture loss.³⁵

Yang *et al.*³⁵ described the effect of both chitosan or oligochitosan as natural antifungal agents against *Monilinia fructicola*, controlling the brown rot of peach, acting in this article as a polymeric material used to produce the capsules and as a natural preservative, contributing positively to antifungal activity. Chitosan also demonstrated ability to control the postharvest decay and elicits defense response in kiwifruit. This edible and eco-friendly material was indicated as an alternative to synthetic fungicides, increasing the total phenolic compounds in kiwifruit, exhibiting an overall beneficial effect on the product quality.³⁶ A wide range of studies describing edible films and coating formulations, containing natural extracts, as antioxidant and antimicrobial activity was reported in literature, as reviewed by Ribeiro *et al.*³⁷

Another factor that may be associated with the superior performance of chitosan-coated NCs is their positive surface charge (ζ -potential: 32 ± 5 mV), which can ionically interact with the negative charge of the fungal membrane phospholipids. This interaction increases membrane permeability causing loss of cell content and leading to fungus death.³⁸ Furthermore, the size of the NCs may also be related to better antifungal activity, as by reducing the size, the contact surface area increases, promoting a better affinity with fungal cells.²⁸

In this way, considering the factors that influence the surface properties of nectarine adherence and antimicrobial activity, the NCs containing eugenol with the outer layer of chitosan (Ne-LbL₁) promoted better adherence and showed the best antimicrobial control. However, the Ne-LbL₂ NCs also showed control of the pathogen, in lesser intensity, but higher or at the level of the commercial fungicide. A previous version of this article has been published as preprint.³⁹

Conclusions

The polymeric nanocapsules containing eugenol proved to be promising for fruit coating in the protection against brown rot caused by *Monilinia fructicola*, to increase fruit storage or shelf life, in addition to using much less toxic natural substances as fungicides.

Supplementary Information

Supplementary information (TGA, image of the macroscopic aspect of treatments and image of the inhibition tests) is available free of charge at <http://jbcs.sbq.org.br> as PDF file.

Acknowledgments

The authors would like to thank Universidade Federal do Paraná (UFPR) for the scientific and technical assistance they provided. The authors would like to thank MSc Rafaele R. Moreira for survival analysis.

J.J., M.J.B.G., N.C.S. and G.P.P. are grateful for the doctoral scholarships received from CAPES (Finance Code 001). R.A.F. (No. 303312/2019-0) and L.L.M.D.M. (306907/2017-8) are Research Members of the National Research Council of Brazil (CNPq). This study was financed by the Coordenação de Aperfeiçoamento de Pessoal de Nível Superior, Brasil (CAPES), coordinated by R.A.F. CAPESPRINT 41/2017 (No. 88887.311748/2018-00) and CNPq (No. 400117/2016-9 and 430451/2018-0).

Author Contributions

J.J. was responsible for formal analysis, investigation, writing original draft; G.P.P. for formal analysis, investigation, writing original draft; M.J.B.G. for formal analysis; N.C.S. for formal analysis; L.L.M.D.M. for conceptualization, funding acquisition, project administration, resources, writing-review and editing; F.A.M. for conceptualization, funding acquisition, project administration, resources, writing-review and editing; R.A.F. for conceptualization, funding acquisition, data curation, project administration, resources, writing-review and editing

References

- Slavin, J. L.; Lloyd, B.; *Adv. Nutr.* **2012**, *3*, 506. [Crossref]
- Lurie, S.; Crisosto, C. H.; *Postharvest Biol. Technol.* **2005**, *37*, 195. [Crossref]
- Xi, Y.; Fan, X.; Zhao, H.; Li, X.; Cao, J.; Jiang, W.; *LWT - Food Sci. Technol.* **2017**, *75*, 537. [Crossref]
- Lino, L. O.; Pacheco, I.; Mercier, V.; Faoro, F.; Bassi, D.; Bornard, I.; Quilot-Turion, B.; *J. Agric. Food Chem.* **2016**, *64*, 4029. [Crossref]
- Keske, C.; Amorim, L.; Mio, L. L. M.; *Crop Prot.* **2011**, *30*, 802. [Crossref]
- May-De Mio, L. L.; Luo, Y.; Michailides, T. J.; *Plant Dis.* **2011**, *95*, 821. [Crossref]
- Garcia-Benitez, C.; Melgarejo, P.; De Cal, A.; *Int. J. Food Microbiol.* **2017**, *241*, 117. [Crossref]
- Hong, C.; Holtz, B. A.; Morgan, D. P.; Michailides, T. J.; *Plant Dis.* **1997**, *81*, 519. [Crossref]
- Pereira, W. V.; Padilha, A. C. N.; Kaiser, J. A. O.; Nesi, C. N.; Fischer, J. M. M.; May-De-Mio, L. L.; *Trop. Plant Pathol.* **2018**, *44*, 120. [Crossref]
- Bakkali, F.; Averbeck, S.; Averbeck, D.; Idaomar, M.; *Food Chem. Toxicol.* **2008**, *46*, 446. [Crossref]
- Khalil, A. A.; Rahman, U.; Khan, M. R.; Sahar, A.; Mehmood, T.; Khan, M.; *RSC Adv.* **2017**, *7*, 32669. [Crossref]
- Rozwalka, L. C.; Moreira, R. R.; Garcia, M. J. B.; Marques, F. A.; May De Mio, L. L.; *J. Phytopathol.* **2020**, *168*, 342. [Crossref]
- Turek, C.; Stintzing, F. C.; *Compr. Rev. Food Sci. Food Saf.* **2013**, *12*, 40. [Crossref]
- Li, W.; Chen, H.; He, Z.; Han, C.; Liu, S.; Li, Y.; *LWT - Food Sci. Technol.* **2015**, *62*, 39. [Crossref]
- Lima, A. L.; Gratieri, T.; Cunha-Filho, M.; Gelfuso, G. M.; *Methods* **2022**, *199*, 54. [Crossref]
- Rao, J. P.; Geckeler, K. E.; *Prog. Polym. Sci.* **2011**, *36*, 887. [Crossref]
- Wang, H.; Qian, J.; Ding, F.; *J. Agric. Food Chem.* **2018**, *66*, 395. [Crossref]
- Dash, M.; Chiellini, F.; Ottenbrite, R. M.; Chiellini, E.; *Prog. Polym. Sci.* **2011**, *36*, 981. [Crossref]
- Zhang, S.; Liu, W.; Liang, J.; Li, X.; Liang, W.; He, S.; Zhu, C.; Mao, L.; *Cellulose* **2013**, *20*, 1135. [Crossref]
- Jacumazo, J.; de Carvalho, M. M.; Parchen, G. P.; Campos, I. M. F.; Garcia, M. J. B.; Brugnari, T.; Maciel, G. M.; Marques, F. A.; de Freitas, R. A.; *Carbohydr. Polym.* **2020**, *230*, 115562. [Crossref]
- Owens, D.; Wendt, R. C.; *J. Appl. Polym. Sci.* **1969**, *13*, 1741. [Crossref]
- Kaelble, D. H.; *J. Adhesion* **1970**, *2*, 66. [Crossref]
- GraphPad Software; *GraphPad Prism*, version 8.0.0 for Windows; California, USA, 2018.
- R version 3.4.3; R Foundation for Statistical Computing, Vienna, Austria, 2018.
- Origin, Microcal Origin 8.0; OriginLab Corp., Northampton, MA, 2009.
- Abbas, S.; Karangwa, E.; Bashari, M.; Hayat, K.; Hong, X.; Sharif, H. R.; Zhang, X.; *Ultrason. Sonochem.* **2015**, *23*, 81. [Crossref]
- Liu, Y.; Yang, J.; Zhao, Z.; Li, J.; Zhang, R.; Yao, F.; *J. Colloid Interface Sci.* **2012**, *379*, 130. [Crossref]

28. Xu, R.; *Particle Characterization: Light Scattering Methods*, 1st ed.; Kluwer Academic Publishers: New York, 2006.
29. Wang, Q.; Zhang, L.; Ding, W.; Zhang, D.; Reed, K.; Zhang, B.; *Food Bioprocess Technol.* **2020**, *13*, 1024. [Crossref]
30. Zambrano-Zaragoza, M. L.; González-Reza, R.; Mendoza-Muñoz, N.; Miranda-Linares, V.; Bernal-Couoh, T. F.; Mendoza-Elvira, S.; Quintanar-Guerrero, D.; *Int. J. Mol. Sci.* **2018**, *19*, 705. [Crossref]
31. Moncayo, D.; Buitrago, G.; Algecira, N.; *Ing. Invest.* **2013**, *33*, 11.
32. Velásquez, P.; Skurtys, O.; Enrione, J.; Osorio, F.; *Food Biophys.* **2011**, *6*, 349. [Crossref]
33. Lino, L. O.; Quilot-Turion, B.; Dufour, C.; Corre, M. N.; Lessire, R.; Génard, M.; Poëssel, J. L.; *J. Exp. Bot.* **2020**, *71*, 5521. [Crossref]
34. Elsabee, M. Z.; Abdou, E. S.; *Mater. Sci. Eng. C* **2013**, *33*, 1819. [Crossref]
35. Yang, L.-Y.; Zhang, J.-L.; Bassett, C. L.; Meng, X.-H.; *LWT - Food Sci. Technol.* **2012**, *46*, 254. [Crossref]
36. Zheng, F.; Zheng, W.; Li, L.; Pan, S.; Liu, M.; Zhang, W.; Liu, H.; Zhu, C.; *Food Bioprocess Technol.* **2017**, *10*, 1937. [Crossref]
37. Ribeiro, A. M.; Estevinho, B. N.; Rocha, F.; *Food Bioprocess Technol.* **2021**, *14*, 209. [Crossref]
38. Devlieghere, F.; Vermeulen, A.; Debevere, J.; *Food Microbiol.* **2004**, *21*, 703. [Crossref]
39. Jacumazo, J.; Parchen, G. P.; Meira J. B.; Ballesteros-Garcia, M. J.; da Silva, N. C.; De Mio, L. L.; Marques, F. A.; de Freitas, R. A.; *Research Square*, 2022. [Link] accessed in January 2023

Submitted: September 17, 2022

Published online: February 8, 2023

